

# Guest-Triggered Zn<sup>II</sup> Translocation and Supramolecular Nuclearity Control in Calix[6]arene-Based Complexes

Nicolas Bernier, Nicolas Menard, Benoit Colasson, Jean-Noël Rebilly,\* and Olivia Reinaud\*

Laboratoire de Chimie et Biochimie Pharmacologiques et Toxicologiques, CNRS UMR 8601, PRES Sorbonne Paris Cité, Université Paris Descartes, 45 rue des Saints Pères, 75006 Paris, France

## Supporting Information

**ABSTRACT:** Two new polytopic ligands based on a calix[6]arene scaffold were synthesized. The truncated cone-shaped calixarene was functionalized at its small rim by a trisimidazole site, aimed at generating a tetrahedral Zn<sup>II</sup> complex, where a fourth labile site inside the cavity is accessible through the funnel provided by its large rim. Tridentate aza ligands (either two or three) were then grafted at this large rim (the entrance of the cavity). Zn<sup>II</sup> coordination studies, monitored by <sup>1</sup>H NMR spectroscopy, showed unprecedented behavior in this family of heteropolytopic ligands. Indeed, it gives access to complexes of various nuclearities in acetonitrile, where zinc binding is under the supramolecular control of the guest. It is first shown that, in the absence of a good guest donor (a primary amine), Zn<sup>II</sup> binding is favored at the large rim where two tridentate nitrogenous groups can form an octahedral complex. The addition of a long guest such as heptylamine induces the quantitative translocation of the Zn<sup>II</sup> ion from the large rim octahedral (O<sub>h</sub>) site to the small rim tetrahedral (T<sub>d</sub>) site provided by the trisimidazole core and the guest ligand. With 2 equiv of Zn<sup>II</sup>, well-defined dinuclear complexes were obtained and isolated, with one Zn<sup>II</sup> ion bound at each rim. Interestingly, it is shown that the binding mode at the large rim is under the supramolecular control of the guest bound at the small rim (with short guests, the O<sub>h</sub> environment is obtained at the large rim, whereas long guests disrupt this core through an induced-fit process); the partially included and dangling alkyl chain opens the large rim (entrance of the cavity) and pushes apart the tridentate moieties. As a result, a guest-induced switch of Zn<sup>II</sup> binding mode occurs and frees one of the tridentate groups from coordination, allowing further extension of the complex nuclearity.



## INTRODUCTION

Metal ions in natural systems can display various roles, ranging from structural and transport to activation of small molecules or electron transfer. Each of these roles is closely related to the nature of the metal ion and its first coordination sphere (Lewis acidity, softness, redox properties, etc.), but it is also greatly influenced by the nature of the second and further spheres, through the presence and nature of substrate binding pockets and access channels.<sup>1,2</sup> In some metallo-enzymes, several metal centers are present with a specific role assigned to each of them, despite similar coordination spheres. For instance, in the copper hydroxylating enzyme peptidylglycine  $\alpha$ -hydroxylating monooxygenase (PHM), Cu<sub>M</sub> activates O<sub>2</sub> in the vicinity of the substrate binding site while Cu<sub>H</sub> transfers an electron to Cu<sub>M</sub> during the course of the catalytic cycle.<sup>3</sup> This role discrimination is connected to the location of binding sites and access channels and, thus, to host–guest interactions.<sup>4</sup> In recent years, we have been using heteropolytopic calix[6]arene scaffolds to generate polynuclear systems.<sup>5,6</sup> In a Cu<sup>I/II</sup>/Zn<sup>II</sup> heterodinuclear system, a rare example of double translocation of metal ions was successfully monitored through an electrochemical input, thanks to the design of the two different metal binding sites at the small and large rim of the calixarene.<sup>7</sup> More

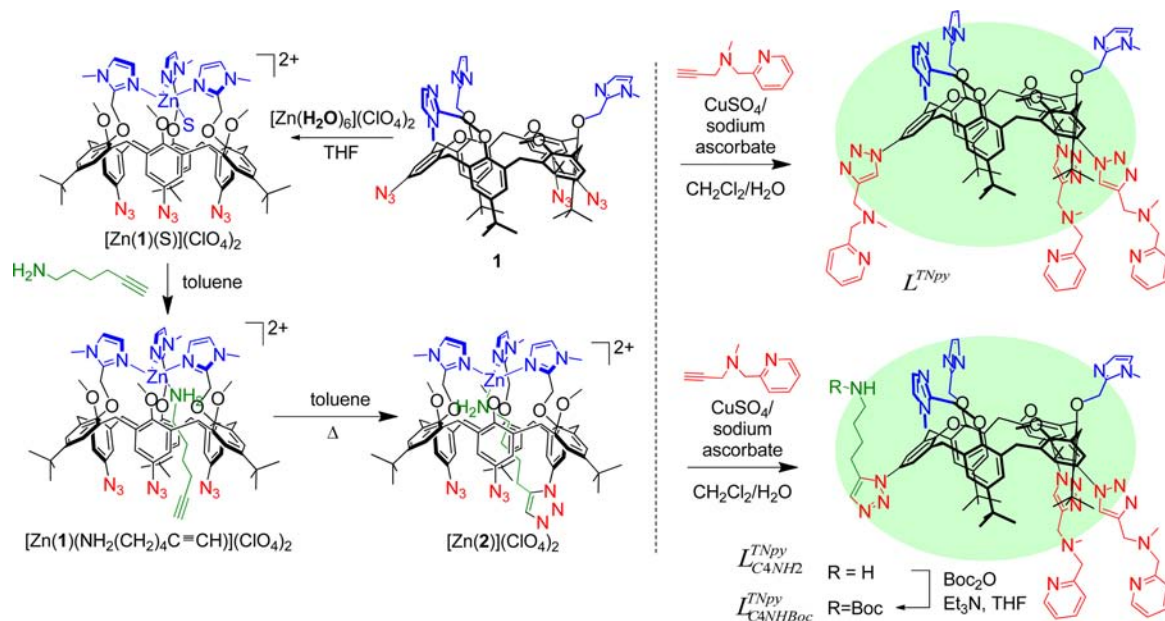
recently, we built a scaffold that allowed us to increase the nuclearity of the complexes with one Zn<sup>II</sup> and three Cu<sup>I</sup> ions selectively bound at the small and large rims, respectively.<sup>8</sup> In all these systems, the first metal ion binding always occurs at the small rim tris-imidazole site, which gives rise to a tetrahedral (T<sub>d</sub>) complex (the so-called “funnel complex”) that is best stabilized.

Herein, we report two new scaffolds for which the mononuclear Zn<sup>II</sup> “resting state” is apparently deprived of host–guest properties in acetonitrile. However, the addition of amine guests induces Zn<sup>II</sup> relocation to the small rim. This chemoselectivity is also associated with size selectivity, as this system leads to a clean translocation for long guests and to a reorganization and encapsulation of the guest between two Zn<sup>II</sup> centers for shorter ones, evidencing a supramolecular control of the coordination properties of these ligands. This supramolecular control is further observed in polynuclear complexes, in which exchange of a small guest (MeCN, propylamine) for a longer one (heptylamine) induces a switch in the coordination mode of the large rim Zn<sup>II</sup> centers.

Received: February 4, 2013

Published: April 3, 2013



Scheme 1. Synthetic Strategies for the Synthesis of  $L^{\text{TNpy}}$  and  $L^{\text{TNpy}}_{\text{C}_4\text{NH}^{\text{Boc}}}$ 

## RESULTS

**Ligand Synthesis.** The calix[6]arene platform bearing three imidazole “arms” at the small rim was functionalized at the large rim using azido/alkyne cycloaddition methodologies to give rise to two different ligands,  $L^{\text{TNpy}}$  and  $L^{\text{TNpy}}_{\text{C}_4\text{NH}^{\text{Boc}}}$  presenting three and two identical tridentate pendant “legs”, respectively (TNpy = [*N*-methyl,*N*-(2-pyridyl-methyl)]-amino-methyl-triazolyl and Boc = *tert*-butyloxycarbonyl). In both cases, the calix[6]arene building block **1** substituted by three azido groups at the large rim was used to graft *N*-(2-pyridyl)-*N*-(4-triazolyl)methylamine units (see Scheme 1).<sup>5</sup>

The synthesis of  $L^{\text{TNpy}}$  was adapted from a strategy reported for a closely related ligand.<sup>8</sup> Calixarene **1** was reacted with an excess of *N*-methyl-*N*-propargyl-2-picolyamine at room temperature in a biphasic  $\text{CH}_2\text{Cl}_2$ /water mixture using  $\text{CuSO}_4$ /NaAsc as a catalyst.<sup>9</sup> Under these conditions,  $L^{\text{TNpy}}$  was obtained as a single product and fully characterized (see Figures S1–S4 in the Supporting Information). Its  $^1\text{H}$  NMR spectrum is displayed in Figure 1. The introduction of bulky substituents at the large rim slows the conformational motion of the macrocycle, leading to broad resonances at room temperature for the calixarene core, whereas sharp peaks for the pyridine substituents are maintained. When recorded at 340 K, the spectrum displays much sharper resonances with a signature attesting to a  $C_{3v}$  symmetrical compound as awaited for a trifunctionalized calix[6]arene.

For the synthesis of the scaffold bearing only two tridentate “legs”, we first tried to decrease the stoichiometry of alkyne versus calixarene **1** used for the copper-catalyzed cycloaddition reaction (<3 equiv). However, it led to a mixture of monofunctionalized, difunctionalized, and trifunctionalized species that we were unable to separate. We thus turned to a different strategy. We have recently described a methodology for the selective monofunctionalization of the calix[6]arene large rim based on the covalent capture of a guest.<sup>10,11</sup> Hence, we used this strategy to first monoreact the tris-azido calixarene large rim, in order to subsequently and selectively graft only two tridentate groups at the large rim. Therefore, the  $\text{Zn}^{\text{II}}$  complex based on ligand **1** was first assembled with an amino

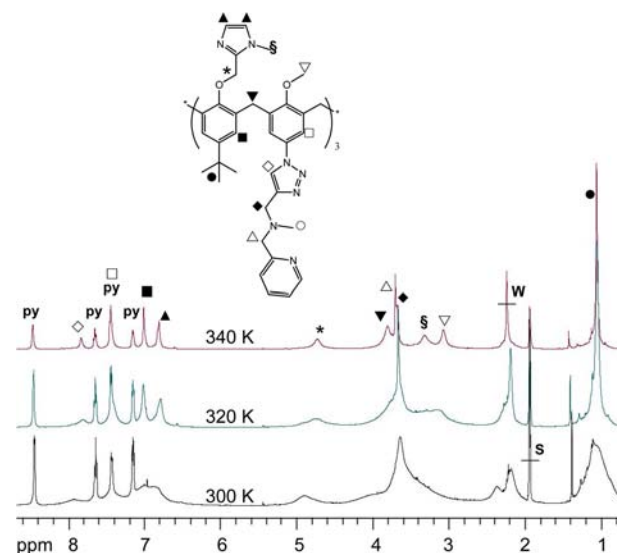


**Figure 1.**  $^1\text{H}$  NMR spectra of  $L^{\text{TNpy}}$  ( $\text{CD}_3\text{CN}$ , 500 MHz) at various temperatures. (“py” indicates the resonances of the pyridyne protons.)

ligand bearing an alkyne function to produce the corresponding host–guest adduct (Scheme 1). Thermal activation then led to the clean cycloaddition of the alkyne moiety with one out of three azido sites of **1**, leaving two available azido groups at the large rim.<sup>10</sup> The latter were subsequently engaged in a copper-catalyzed cycloaddition similar to that used for  $L^{\text{TNpy}}$  to give  $L^{\text{TNpy}}_{\text{C}_4\text{NH}_2}$ . Finally, the coordination ability of the primary amine was neutralized by Boc protection, and the new ligand  $L^{\text{TNpy}}_{\text{C}_4\text{NH}^{\text{Boc}}}$  was obtained.  $L^{\text{TNpy}}_{\text{C}_4\text{NH}^{\text{Boc}}}$  was fully characterized by NMR spectroscopy in dimethylsulfoxide (DMSO), and showed temperature dependence similar to that of  $L^{\text{TNpy}}$  in  $\text{CD}_3\text{CN}$  but, at 340 K, yielded a spectrum reflecting a lower symmetry ( $C_s$ ) (see Figures S13–S17 in the Supporting Information).

The coordination of these new scaffolds toward  $\text{Zn}^{\text{II}}$  and the host–guest behavior of the resulting complexes were then studied, first by associating 1 equiv of metal ion to the platform, and then by extending the complexes nuclearity, in order to

explore differences with the behavior of previously reported parent hosts.<sup>5,8</sup>

**Characterization of Zn<sup>II</sup> Complexes. Formation of a Mononuclear Host–Guest Adduct.** The addition of 1 equiv of Zn<sup>II</sup> to a CD<sub>3</sub>CN solution of L<sup>TNpy</sup> considerably sharpened the <sup>1</sup>H NMR resonances, with respect to the free ligand (Figure 2).

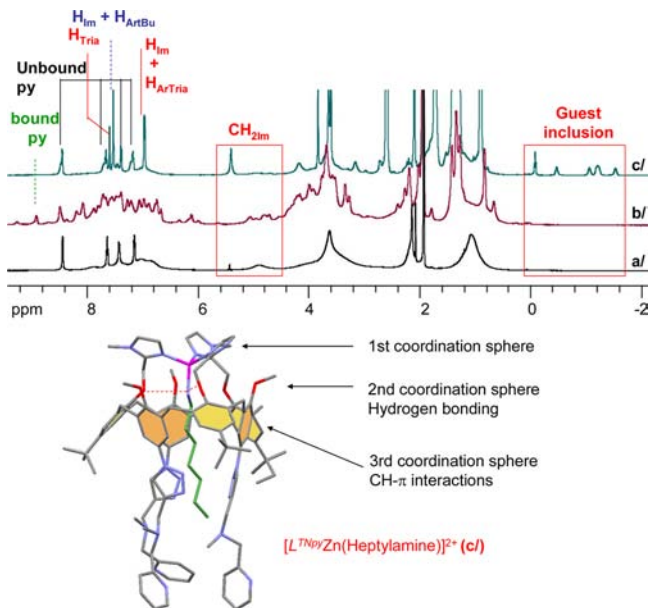


**Figure 2.** (Top) <sup>1</sup>H NMR spectra (CD<sub>3</sub>CN, 500 MHz, 300 K) obtained for a 1:1 L<sup>TNpy</sup>:Zn<sup>II</sup> stoichiometry: (a) L<sup>TNpy</sup>, (b) L<sup>TNpy</sup> + 1 equiv Zn(OTf)<sub>2</sub>, and (c) L<sup>TNpy</sup> + 1 equiv Zn(OTf)<sub>2</sub> + 4 equiv heptylamine (TfO<sup>-</sup> is a triflate counterion (trifluorosulfonate)). (Bottom) Representation of the mononuclear host–guest adduct (funnel complex)<sup>12</sup> identified from spectrum (c).

However, it yielded an extremely complex spectrum, which suggests the formation of a mixture of species deprived of symmetry (Figure 2b). The pyridine resonance changes indicated some coordination of Zn<sup>II</sup> at the large rim sites. Indeed, the intensity of the ortho proton of the free pyridine (8.5 ppm) decreased in favor of a new resonance at 8.9 ppm, corresponding to the expected value for the ortho proton of a bound pyridine moiety. A similar behavior was observed for L<sup>TNpy</sup><sub>C<sub>4</sub>NHBoc</sub> (see Figure S18 in the Supporting Information). A structure of these compounds will be proposed in the “polynuclear species” section (vide infra). Upon the addition of heptylamine to the previous solution, the initial signals progressively disappeared in favor of a new set of peaks, corresponding to a new species in slow exchange (on the NMR time scale) with the starting one. Full conversion was almost reached with 1 equiv of heptylamine. This new species displays a C<sub>3v</sub> symmetry, as attested by a single *t*-Bu resonance (see Figure 2c).<sup>13</sup> In particular, the CH<sub>2</sub>Im resonances appear as a single peak that is shifted downfield, which indicates coordination of Zn<sup>II</sup> at the small rim. This is further confirmed by the resonances in the [0, –2 ppm] window, which correspond to the heptylamine bound inside the cavity. Finally, the pyridine and triazole signals are observed at chemical shifts corresponding to unbound groups. All these data are in agreement with the formation of a funnel complex<sup>12</sup> with a heptylamine guest bound inside the cavity (Figure 2), as previously reported for the parent calix[6]arene tris-imidazole ligand bearing six *t*-Bu substituents at the large rim.<sup>14</sup> With

ligand L<sup>TNpy</sup><sub>C<sub>4</sub>NHBoc</sub> of lower symmetry (C<sub>s</sub>), the corresponding host–guest adduct was also obtained with 1 equiv of Zn<sup>II</sup> and heptylamine (see Figure S18 in the Supporting Information).

**Dinuclear Complex with a Small Guest: Octahedral Coordination at the Large Rim.** The addition of 2 equiv of Zn<sup>II</sup> to L<sup>TNpy</sup> in CD<sub>3</sub>CN yielded a single species, as attested by the very well-defined and fully attributed <sup>1</sup>H NMR spectrum (see Figure 3 and Figures S19–S21 in the Supporting

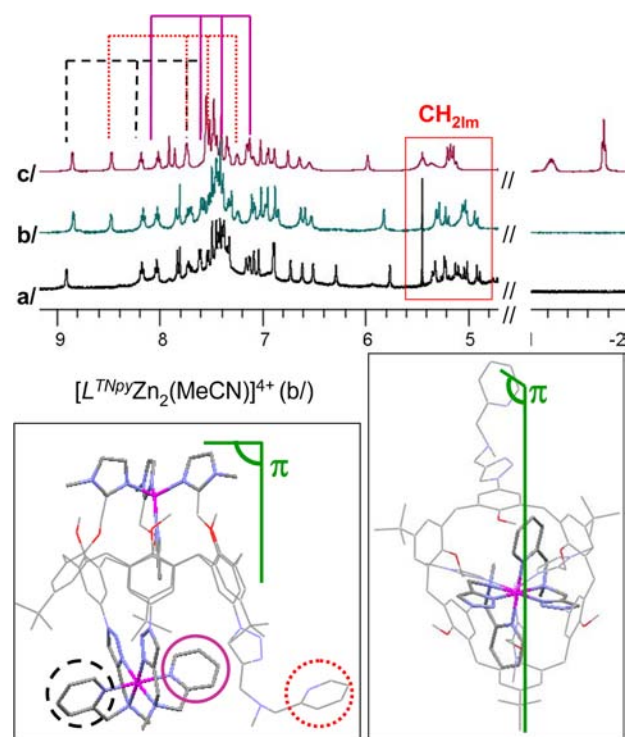


**Figure 3.** (Top) Comparative <sup>1</sup>H NMR spectra (CD<sub>3</sub>CN, 265 K, 500 MHz) of (a) L<sup>TNpy</sup><sub>C<sub>4</sub>NHBoc</sub>Zn<sub>2</sub>(MeCN)(ClO<sub>4</sub>)<sub>4</sub>, (b) L<sup>TNpy</sup>Zn<sub>2</sub>(MeCN)-(ClO<sub>4</sub>)<sub>4</sub>, and (c) L<sup>TNpy</sup>Zn<sub>2</sub>(propylamine)(ClO<sub>4</sub>)<sub>4</sub>. (Bottom) Proposed structure for complex L<sup>TNpy</sup>Zn<sub>2</sub>(MeCN)(ClO<sub>4</sub>)<sub>4</sub> side view (left) and upper view (right).

Information). The corresponding complex with its dangling tridentate group in protonated form, [L<sup>TNpy</sup>Zn<sub>2</sub>(MeCN)-(OTf)<sub>4</sub>(TfOH)], could actually be isolated and characterized (see the Supporting Information). The <sup>1</sup>H NMR key features are as follows:

- The *t*-Bu substituents give rise to two peaks of 1:2 intensity ratio. This is indicative of a C<sub>s</sub> symmetry for the complex, where the π-symmetry plane contains the cone “axis” and one of the *t*-Bu groups (see Figure S21 in the Supporting Information).
- The overall downfield shift observed for the CH<sub>2</sub>Im resonances upon the addition of the second equivalent of Zn<sup>II</sup> is consistent with the coordination of the three imidazole groups (Figure 3b). One Zn<sup>II</sup> center is thus located at the small rim and included in the π-symmetry plane. The nonsymmetrical CH<sub>2</sub>Im pattern is reminiscent of previously reported funnel complexes of C<sub>s</sub> symmetry.<sup>10</sup>
- COSY experiments (Figure S19 in the Supporting Information) indicate three distinct sets of pyridine peaks. One set of resonances correspond to one unbound pyridine moiety, another set of resonances



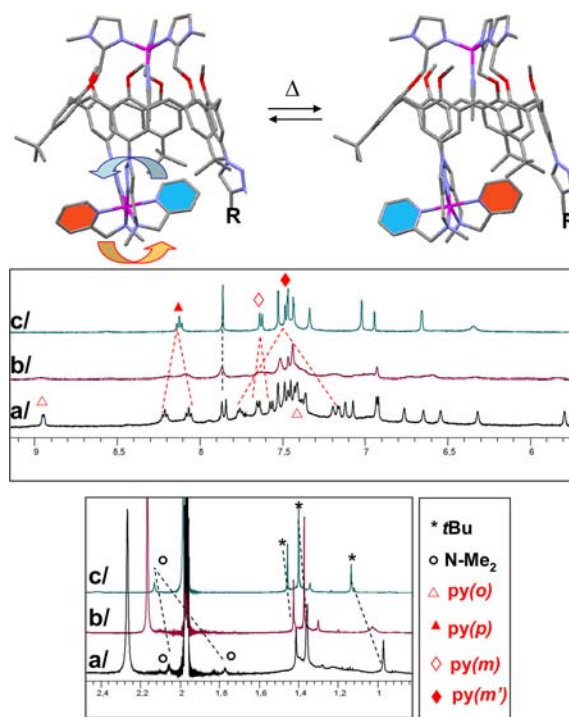
- stems for a “classical” bound pyridine, whereas the last one is shifted highly upfield, with respect to the other two. This suggests that the corresponding pyridine moiety is projected toward the inside of the cavity and is shielded by the aromatic walls.
- One  $\text{Zn}^{\text{II}}$  ion is thus located at the small rim and the second  $\text{Zn}^{\text{II}}$  ion is bound to (at least) one tridentate TNpy group. These two ions are necessarily included in the  $C_s$  symmetry plane in order to explain the observed symmetry.
  - In this  $C_s$  symmetry, two pyridine sets of resonances in a 1:2 ratio are expected, except in the specific case where all three pyridines are included in the symmetry plane. In this situation, three distinct sets of peaks can be obtained, which corresponds to the experimental observation. In order to constrain all pyridines in the same plane, both the “bound” and the “intracavity” pyridine groups must be simultaneously coordinated to a single  $\text{Zn}^{\text{II}}$  ion.

Basic geometry optimization using Hyperchem confirmed that such a binding mode forces one pyridine group out of the cavity (the “classical” bound pyridine) and the other inside the cavity (the shielded “intracavity” pyridine), as depicted in Figure 3. The resulting octahedral ( $O_h$ ) complex appears almost symmetrical, with respect to the  $\pi$ -mirror plane. As a consequence, all groups located away from the  $O_h$   $\text{Zn}^{\text{II}}$  center (such as the *t*-Bu groups) sense a  $C_s$  symmetry, whereas those lying in the vicinity of the complex ( $H_{\text{ArTri}}$  for instance; see Figures S19–S21 in the Supporting Information) sense an effective symmetry descent to group  $C_1$  and their resonances appear fully split.

If this hypothesis is correct, a similar pattern should be observed with  $L_{\text{C}_4\text{NHBoc}}^{\text{TNpy}}$ , since its two tridentate ligands at the large rim can also form the same octahedral environment, with the Boc-protected side chain of  $L_{\text{C}_4\text{NHBoc}}^{\text{TNpy}}$  playing a spectator role, like the third tridentate leg in  $L^{\text{TNpy}}$ . We thus recorded the spectra of both systems at 265 K, because the resonances are significantly sharper at this temperature.

The  $^1\text{H}$  NMR spectra of  $L^{\text{TNpy}}\text{Zn}_2(\text{MeCN})(\text{ClO}_4)_4$  and  $L_{\text{C}_4\text{NHBoc}}^{\text{TNpy}}\text{Zn}_2(\text{MeCN})(\text{ClO}_4)_4$  (Figure 3) show very similar chemical shifts, except for the signals of the unbound tridentate group, which is replaced by the Boc protected chain in  $L_{\text{C}_4\text{NHBoc}}^{\text{TNpy}}\text{Zn}_2(\text{MeCN})(\text{ClO}_4)_4$ . Full attribution of the resonances for  $L^{\text{TNpy}}\text{Zn}_2(\text{MeCN})(\text{ClO}_4)_4$  and  $L_{\text{C}_4\text{NHBoc}}^{\text{TNpy}}\text{Zn}_2(\text{MeCN})(\text{ClO}_4)_4$  was carried out by correlation spectroscopy (COSY) and heteronuclear single quantum coherence (HSQC) experiments (see Figures S19–S25 in the Supporting Information). The  $\text{Zn}^{\text{II}}$  coordination mode at the large rim is thus confirmed by comparison of selected resonances ( $H_{\text{Tri}}$ ,  $H_{\text{py}}$ ,  $H_{\text{NMe}}$ ) in the free ligand and the complex (see Table S1 in the Supporting Information). The dinuclear complex was also detected by ESI-MS spectrometry (see the Supporting Information).

To further confirm this attribution, the complex  $L_{\text{C}_4\text{NHBoc}}^{\text{TNpy}}\text{Zn}_2(\text{MeCN})(\text{ClO}_4)_4$  was studied within the temperature range of 275–340 K in  $\text{CD}_3\text{CN}$  (via  $^1\text{H}$ , COSY, HSQC; see Figure 4 and Figures S26 and S27 in the Supporting Information). The two sets of pyridine resonances observed at 275 K merged into coalescence at 340 K.<sup>15</sup> This coalescence is indicative of an exchange phenomenon that is slow at 275 K and fast at 340 K (on the NMR time scale). The endo and the exo pyridine groups are switching roles, i.e., the helicity of the large rim complex is inverted, as schematized in Figure 4.

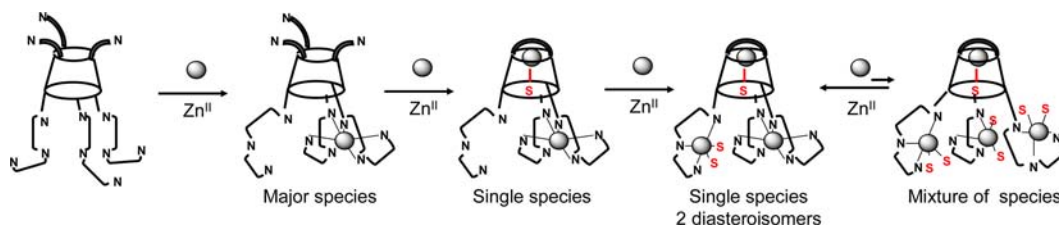
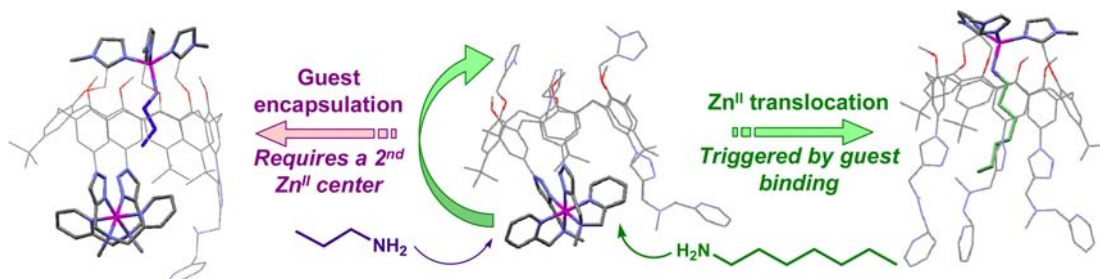


**Figure 4.** Selected  $^1\text{H}$  NMR ( $\text{CD}_3\text{CN}$ , 500 MHz) spectra of  $L_{\text{C}_4\text{NHBoc}}^{\text{TNpy}}\text{Zn}_2(\text{MeCN})(\text{ClO}_4)_4$  at (a) 275 K, (b) 300 K, and (c) 340 K. Correlations are indicated in dotted lines.  $R = \text{C}_4\text{H}_8\text{NHBoc}$ .

The structure of the dinuclear complex of  $L^{\text{TNpy}}$  also enlightens, in hindsight, the nature of the main species obtained with 1 equiv of  $\text{Zn}^{\text{II}}$  (see Figure S28 in the Supporting Information). Indeed, the pyridine pattern of the main species observed with one  $\text{Zn}^{\text{II}}$  ion is reminiscent of that observed for  $L^{\text{TNpy}}\text{Zn}_2(\text{MeCN})(\text{ClO}_4)_4$ , suggesting a similar  $O_h$  environment for the  $\text{Zn}^{\text{II}}$  center bound at the large rim. Furthermore, the corresponding to the  $\text{CH}_2\text{Im}$  protons is shifted upfield, which is indicative that no  $\text{Zn}^{\text{II}}$  center is bound at the small rim. Similar conclusions can be drawn in the case of  $L_{\text{C}_4\text{NHBoc}}^{\text{TNpy}}$  (see Figure S22 in the Supporting Information). The structure depicted in Schemes 2 and 3 can thus be proposed for the main mononuclear complex  $L^{\text{TNpy}}\text{Zn}(\text{ClO}_4)_2$  present in solution.

**Third Equivalent of  $\text{Zn}^{\text{II}}$  Added to  $L^{\text{TNpy}}$ : Formation of a Trinuclear Species—Diastereoisomery.** When a third equivalent of  $\text{Zn}^{\text{II}}$  was added to  $L^{\text{TNpy}}$ , the overall pattern remained close to that of  $L^{\text{TNpy}}\text{Zn}_2(\text{MeCN})(\text{ClO}_4)_4$ , but the resonances of the dangling tridentate ligand were shifted downfield, which is indicative of the coordination of  $\text{Zn}^{\text{II}}$  to the last chelating group (see Figure 5, Figures S28 and Figures S31–33 in the Supporting Information). In fact, two species were obtained, as revealed by the split of various resonances (Figure 5). This is explained by the formation of a new trinuclear complex derived from  $L^{\text{TNpy}}\text{Zn}_2(\text{MeCN})(\text{ClO}_4)_4$ , which exists as a mixture of two diastereoisomers. Indeed, the third  $\text{Zn}^{\text{II}}$  center is bound to the remaining tridentate group (Figure 5), which induces coiling of this tridentate ligand around the metal ion and generates local chirality at both  $\text{Zn}^{\text{II}}$  centers at the large rim.

With complex  $L_{\text{C}_4\text{NHBoc}}^{\text{TNpy}}\text{Zn}_2(\text{MeCN})(\text{ClO}_4)_4$ , the addition of a third equivalent of  $\text{Zn}^{\text{II}}$  in  $\text{CD}_3\text{CN}$  led to a new spectrum in which the resonances between 5.5 ppm and 6.5 ppm ( $H_{\text{ArTri}}$ ) have disappeared (see Figure S22 in the Supporting Information). This is indicative of cavity opening and suggests that the  $O_h$  binding site at the large rim breaks in order to

Scheme 2. Sequential Coordination of  $\text{Zn}^{\text{II}}$  to  $\text{L}^{\text{TNpy}}$  and Formation of a Trinuclear Species  $[\text{L}^{\text{TNpy}}\text{Zn}_3(\text{MeCN})]^{6+}$ Scheme 3. Guest-Selective  $\text{Zn}^{\text{II}}$  Translocation within  $\text{L}^{\text{TNpy}}\text{Zn}(\text{ClO}_4)_2$  (right) and Encapsulation within  $\text{L}^{\text{TNpy}}\text{Zn}_2(\text{MeCN})(\text{ClO}_4)_4$ <sup>a</sup>

<sup>a</sup>Guest = heptylamine, versus propylamine.

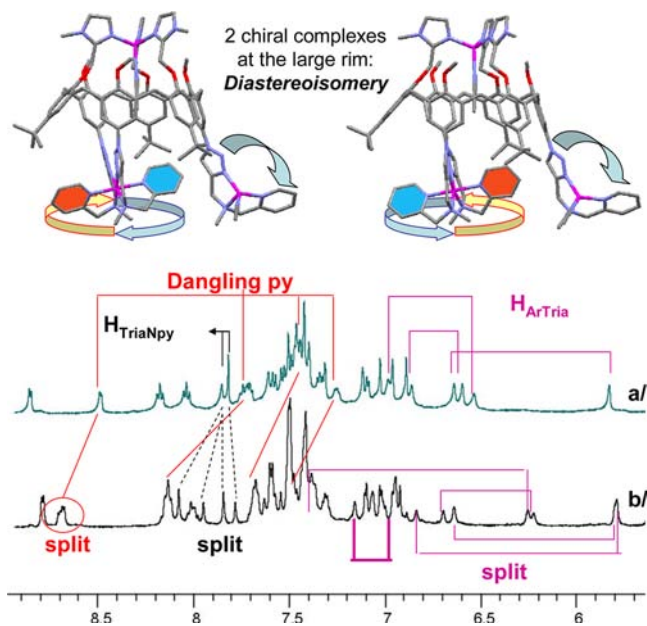


**Figure 5.** Comparison of  $^1\text{H}$  spectra ( $\text{CD}_3\text{CN}$ , 500 MHz, 285 K) of (a)  $\text{L}^{\text{TNpy}}\text{Zn}_2(\text{MeCN})(\text{ClO}_4)_4$  and (b) that obtained via the addition of 3 equiv of  $\text{Zn}^{\text{II}}$  to  $\text{L}^{\text{TNpy}}$ , i.e., the formation of  $[\text{L}^{\text{TNpy}}\text{Zn}_3(\text{MeCN})(\text{ClO}_4)_6]^{6+}$ . The arrows on the molecular models indicate the coiling direction of the tridentate ligand (view along the “cone” axis).

accommodate two  $\text{Zn}^{\text{II}}$  centers, each being bound to a different tridentate group.

With ligand  $\text{L}^{\text{TNpy}}$ , an increased resistance of the  $\text{O}_h$  site is observed. Indeed, addition of a fourth equivalent of  $\text{Zn}^{\text{II}}$  was not enough to fully disrupt this  $\text{O}_h$  core and only after the addition of at least four extra equivalents of  $\text{Zn}^{\text{II}}$  did the  $[\text{L}^{\text{TNpy}}\text{Zn}_3(\text{MeCN})]^{6+}$  NMR signature disappear in favor of a mixture of species with an “open” cavity (no  $\text{H}_{\text{ArTria}}$  resonances in the 5.5–6.5 ppm window). The increased resistance of the  $\text{O}_h$  complex to the addition of excess  $\text{Zn}^{\text{II}}$  in  $\text{L}^{\text{TNpy}}$  vs  $\text{L}_{\text{C}_4\text{NH}_8\text{Boc}}^{\text{TNpy}}$

can be explained using statistical considerations (see Figure S29 in the Supporting Information).

$\text{Zn}^{\text{II}}$  coordination thus occurs sequentially in the order depicted in Scheme 2. The first equivalent is located at the large rim in an  $\text{O}_h$  environment made of two “TNpy” tridentate groups. The second equivalent is located at the  $\text{T}_d$  site provided by the small rim, thus encapsulating a small MeCN guest between the two metal ions. The third equivalent binds to the remaining tridentate “TNpy” group. The formation of species of higher nuclearity requires the breaking of the particularly stable  $\text{O}_h$   $\text{Zn}^{\text{II}}$  complex at the large rim; thus, a great excess of  $\text{Zn}^{\text{II}}$  must be added.

**Guest-Induced Switches. 1:1 Calix[6]arene/ $\text{Zn}^{\text{II}}$  Stoichiometry: Selective  $\text{Zn}^{\text{II}}$  Translocation.** Within the  $[\text{L}^{\text{TNpy}}\text{Zn}]^{2+}$  complex, MeCN is too weak of a ligand to stabilize  $\text{Zn}^{\text{II}}$  in a  $\text{T}_d$  environment at the small rim, and  $\text{O}_h$  binding of two tridentate groups is predominantly observed. However, the site preference remains highly guest-dependent. When a good guest ligand is available (heptylamine, vide supra), the binding strength of  $\text{Zn}^{\text{II}}$  at the  $\text{T}_d$  site of the small rim is enhanced and the metal ion relocates at the imidazole site (Figure 2). The competition terms between the two sites ( $\text{O}_h$  binding at the large rim versus  $\text{T}_d$  “tris-imidazole + guest” at the small rim) are modified because primary amines are stronger donors than MeCN.

However, whereas heptylamine leads to a clean  $\text{Zn}^{\text{II}}$  translocation in mononuclear complexes, a different behavior is observed with a shorter guest such as propylamine: the coordination system self-rearranges to yield predominantly a dinuclear host–guest adduct (vide infra) for low guest: $\text{L}^{\text{TNpy}}\text{Zn}^{\text{II}}$  stoichiometries (see Scheme 3). Equilibria are displaced in favor of the mononuclear adduct only at high guest concentrations (>10 equiv with  $\text{L}^{\text{TNpy}}$ ; see Figure S34 in the Supporting Information). Indeed, depending on the guest length, the tridentate groups at the large rim of this host–guest mononuclear complex are either pushed apart (longer guest heptylamine) or remain in relative close proximity (small guest propylamine). In the former case, the  $\text{O}_h$  binding mode is disrupted through an induced-fit process. In the latter case, the



cavity can wrap around the small guest without disturbing the  $O_h$  site, making subsequent  $Zn^{II}$  coordination much more favorable than the simple translocation that could have been expected. At higher guest concentrations, the mononuclear adduct becomes favored by the law of mass action. A similar behavior was observed for  $L_{C4NHBOc}^{TNpy}$  (see Figure S35 in the Supporting Information).

**1:2 Calix[6]arene/ $Zn^{II}$  Stoichiometry: Selective Disruption of  $Zn^{II}$  Octahedral Binding.** Propylamine (4 equiv) was added to  $L^{TNpy}Zn_2(MeCN)(ClO_4)_4$  and complexation was monitored by  $^1H$  NMR spectroscopy (Figure 3). A single species was obtained, which displays a spectrum that is highly reminiscent of  $L^{TNpy}Zn_2(MeCN)(ClO_4)_4$  (see Figures 3b and 3c). In particular, the patterns in the aromatic region are almost superimposable. The main difference resides in the peaks in the  $[0, -2\text{ ppm}]$  window and the shifted  $H_{CH2Im}$  massif. It can be concluded that propylamine became bound inside the cavity, replacing MeCN, with no perturbation of the  $O_h$  complex at the large rim and that  $L^{TNpy}Zn_2(propylamine)(ClO_4)_4$  (represented in Scheme 3, left) was cleanly produced (see Figure S29 in the Supporting Information).

Reaction of  $L^{TNpy}Zn_2(MeCN)(ClO_4)_4$  with the longer guest heptylamine was also studied in  $CD_3CN$  (see Figure 6). Similar to that observed in the propylamine case, heptylamine readily replaced MeCN as a guest ligand, as attested by the appearance of multiple peaks in the  $[0, -2\text{ ppm}]$  region. However, unlike

the propylamine case, several host–guest species were obtained. This was associated with the disruption of the  $O_h$  site, as shown by the loss of the pyridine and triazole  $O_h$  coordination pattern in the aromatic region. Instead, a massif corresponding to resonances of bound pyridines is found at 8.05 ppm. These observations suggest that the long guest heptylamine prevents the preorganization of TNpy tridentate groups for  $O_h$  binding by pushing apart the triazole moieties. This phenomenon, already observed on previous parent systems,<sup>8</sup> is a consequence of the induced fit, which prevents simultaneous binding of two triazole groups to a single metal ion. The structures of Figure 6 can thus be proposed.

Subsequent addition of  $Zn^{II}$  (third and fourth equivalents) continues to affect the free pyridine signals, indicating further coordination at the large rim.

Note that, although more than four extra equivalents of  $Zn^{II}$  were necessary to convert the trinuclear complex of  $L^{TNpy}$  into a tetranuclear one with MeCN as a guest, only one is required when heptylamine is bound. Hence, by disrupting the stable large rim  $O_h$  core, heptylamine facilitates further  $Zn^{II}$  binding to the three pendant donors. A similar behavior was observed with extended guests (*n*-octadecylamine; see Figure S36 in the Supporting Information).

## DISCUSSION

The ability of the calixarene scaffold to stabilize host–guest systems of high nuclearity is strongly dependent on the nature of the large rim groups and their denticity in particular. Comparison of three systems bearing monodentate, bidentate, and tridentate ligands at the large rim (Scheme 4) highlights several key points that are exposed below.

**$Zn^{II}$  Coordination Site Selectivity: Denticity Versus Second and Third Coordination Sphere Effects.** In the first heteroditopic scaffold that we have reported,  $L^{TOAr}$  (Scheme 4),<sup>5</sup> two binding sites are competitive: a “tris-imidazole” one at the small rim and a “tris-triazole” one at the large rim. In agreement with the better donor ability of imidazole, metal binding preferentially occurs at the small rim. This first binding event organizes the triazole groups at the large rim in a cofacial manner and a second metal ion can be subsequently bound at the large rim.

Increasing the denticity at the large rim led to  $L^{TNMe2}$ , bearing three bidentate aminomethyl-triazole legs.<sup>8</sup> Based on ligand-donating properties, binding at the large rim should be favored, as an  $N_6$  environment (large rim) should stabilize a Lewis acidic center better than a  $T_d$  site (small rim). However,  $Zn^{II}$  binds preferentially at the small rim, completing its coordination sphere with acetonitrile. This unexpected location was ascribed to the specific preorganization of the small rim site that is absent at the large rim and to the host–guest interactions between MeCN and the cavity. These supramolecular aspects allow the enthalpic gain associated with the higher donor number at the large rim to be overcome.

Increasing the denticity further with tridentate groups ( $L^{TNpy}$ ) changes the binding site preference. With  $L^{TNpy}$  (and  $L_{C4NHBOc}^{TNpy}$ ), the first equivalent of  $Zn^{II}$  invariably locates at the large rim. This behavior is unprecedented in the family of triazole-functionalized compounds. The enthalpic preference for an  $O_h$  environment over the  $T_d$  site provided by three imidazole groups and one acetonitrile is not compensated by the small rim preorganization and guest encapsulation.

However, the addition of a good and long guest donor (heptylamine) switches the coordination back to the small rim,

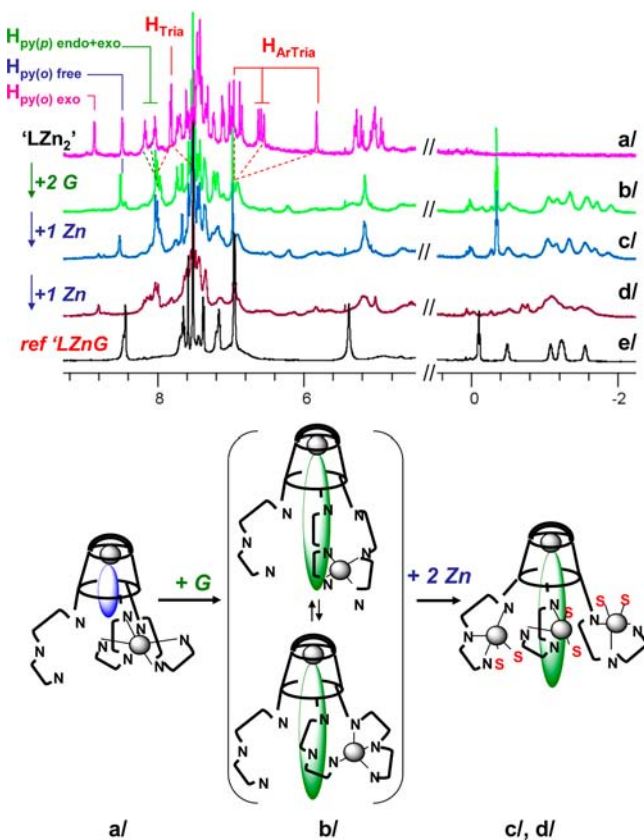
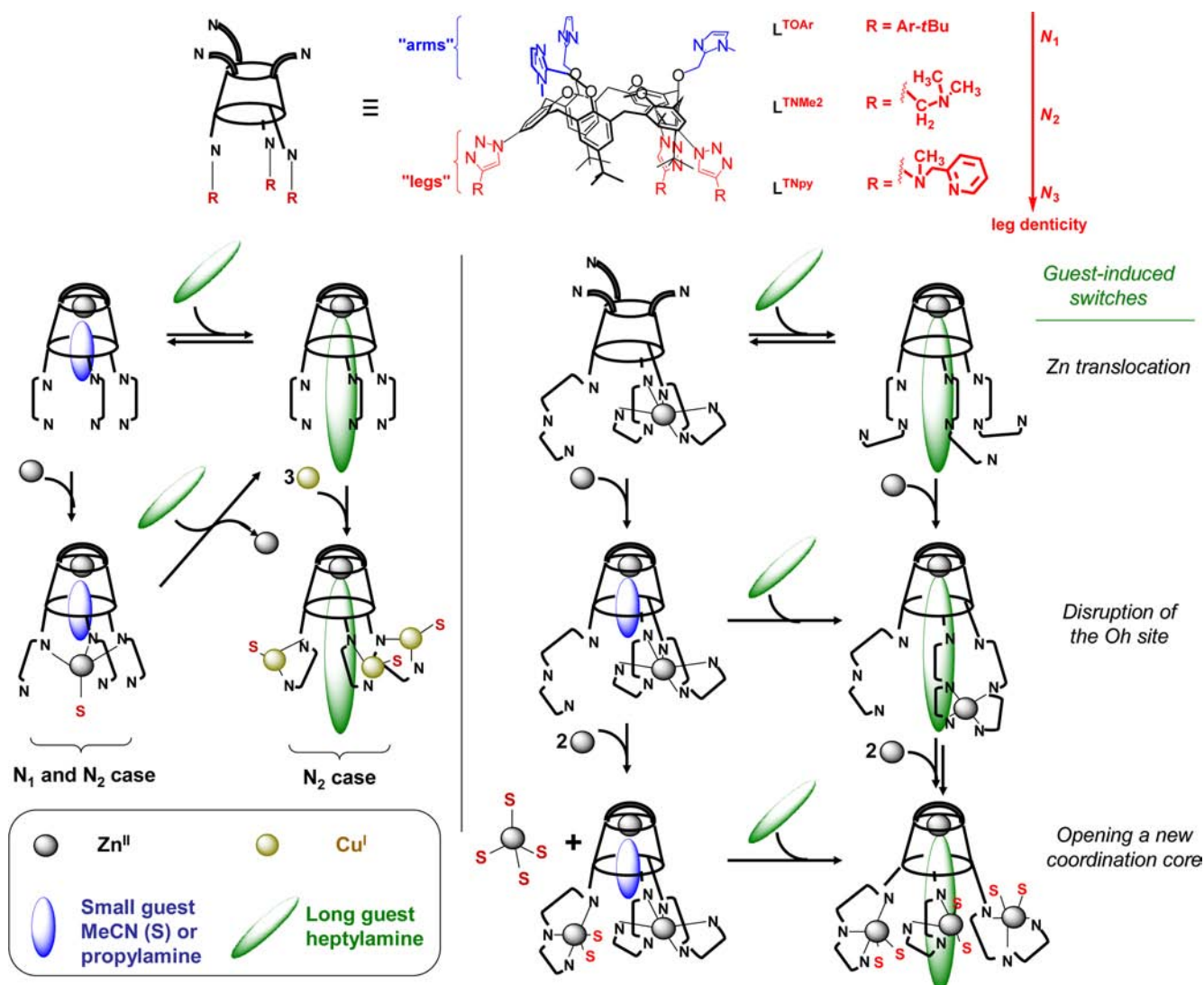


**Figure 6.**  $^1H$  NMR spectra (500 MHz, 280 K,  $CD_3CN$ ) of (a)  $L^{TNpy}Zn_2(MeCN)(ClO_4)_4$ , (b) + 2 equiv of heptylamine, (c) + 2 equiv of heptylamine + 1 equiv  $Zn^{II}$ , (d) 2 equiv of heptylamine + 2 equiv  $Zn^{II}$ , (e) reference spectrum of  $L^{TNpy}Zn(heptylamine)(ClO_4)_2$ . Bottom: schematized structures suggested by the spectra changes ( $L = L^{TNpy}$ ,  $G =$  heptylamine).

Scheme 4. Coordination Properties of Calix[6]arene-based Polytopic Ligands and Host–Guest Behaviors Illustrating the Supramolecular Control on Geometry and Nuclearity of the Corresponding Metal Complexes



yielding the traditional host–guest adduct observed for  $L^{TOAr}$  and  $L^{TNMe_2}$ . The  $T_d$  site becomes preferred over the  $O_h$  site. The main driving force for this switch into the host–guest adduct resides in multiple factors: (i) formation of a  $\text{Zn}^{II}$ –amine coordination bond; (ii) second sphere interactions, thanks to hydrogen bonds developing between the included amine and the crown of O atoms present at the small rim;<sup>14</sup> (iii) third sphere interactions, as multiple  $\text{CH}-\pi$  bonds develop between the alkyl chain of the included guest and the aromatic walls of the calixarene; and (iv) steric perturbation of the  $O_h$  coordination site by the guest alkyl chain dangling at the large rim.

**Induced Fit.** Coordination of an amine guest inside the cavity of a funnel complex involves the three major interactions described above. Because of the flexibility of calix[6]arenes, and in order to maximize such interactions, the cavity wraps around the guest through an induced-fit process. Consequently, the degree of large rim “opening” depends on the size of the guest that is bound at the small rim. For small guests such as MeCN or propylamine, the three triazole groups are brought in the vicinity of each other and preorganized in a cofacial manner. For longer guests such as heptylamine, the triazole groups are

pushed apart and the cofacial arrangement is lost at the large rim. This phenomenon is a key in the guest responsive behavior of these systems and has drastic consequences on the coordination and nuclearity.

**Nuclearity Control. Small Guests: Cofacial Triazole Preorganization.** In  $L^{TOAr}$  and  $L^{TNMe_2}$ ,  $\text{Zn}^{II}$  binds first at the small rim. With a small guest in the cavity, the cofacial “tris-triazole” motif favors a subsequent metal complexation in a  $T_d$  environment, with a solvent molecule completing the coordination sphere (see Scheme 4).<sup>5,8,16</sup> The preorganization prevents further metal binding, even in the presence of extra metal ions. The maximum nuclearity in these two scaffolds is thus limited to two in the presence of a small guest (e.g., MeCN). To increase the nuclearity despite the cofacial preorganization, denticity must be higher. Indeed, with  $L^{TNpy}$ -bearing tridentate groups, a new binding mode is favored, leading to the large rim octahedral core. In the presence of 1 equiv of  $\text{Zn}^{II}$ , neither the tris-imidazole site nor the tris-triazole motif can compete with the chelate effect of the tridentate legs bearing stronger donors. The preferred binding mode thus involves two tridentate groups, taking advantage of both the chelate effect and the preorganization of triazoles. This  $O_h$

arrangement leaves a tris-imidazole core at the small rim and an available  $N_3$  ligand at the large rim that can also bind  $Zn^{II}$  to reach a higher nuclearity (three). Thus, increasing denticity enables further coordination, despite the triazole preorganization.

**Large Guests: Breaking the Cofacial Arrangement.** When heptylamine is anchored at the small rim, the cavity opens and the triazole groups are pushed apart and cannot bind to the same metal ion anymore. In  $L^{TOAr}$ , a single triazole is not a sufficient donor to complex metal ions via a single binding site, and nuclearity of the host–guest adducts is limited to one. In  $L^{TNMe_2}$ , each bidentate  $TNMe_2$  leg at the large rim can bind a metal ion at the very condition that it is not too Lewis acidic. Indeed, tetranuclear species could be stabilized only with  $Cu^I$  ( $[L^{TNMe_2}Zn(heptylamine)Cu^I_3]^{3+}$ ), not with  $Zn^{II}$ . Hence, in the presence of a long guest, an increased denticity is required to bind  $Zn^{II}$  centers at the large rim. In  $L^{TNpy}$ , each tridentate  $TNpy$  group can stabilize a  $Zn^{II}$  ion and polynuclear  $Zn^{II}$  host–guest adducts (nuclearity  $\geq 3$ ) can be obtained.

Nuclearity is thus mainly controlled by two factors:

- The large rim opening, which is controlled by the nature of the guest anchored at the small rim: guest exchange can trigger switches from dinuclearity to mononuclearity ( $L^{TOAr}$ ), dinuclearity to tetranuclearity ( $L^{TNMe_2}$ ), or trinuclearity to tetranuclearity ( $L^{TNpy}$ ).
- The denticity at the large rim: in adducts including long guests,  $L^{TNMe_2}$  can bind  $Cu^I$  at the large rim, while  $L^{TOAr}$  cannot;  $L^{TNpy}$  can bind  $Zn^{II}$  at the large rim, while  $L^{TNMe_2}$  cannot.

Therefore, a fine tuning of the homonuclearity or heteronuclearity is obtained by playing on these two parameters.

## CONCLUSION

Two new heteropolytopic ligands based on a calix[6]arene scaffold were synthesized, bearing either two or three tridentate aza groups at the large rim. Comparison with parent compounds evidenced an unprecedented coordination behavior in this family of complexes for which host–guest properties and nuclearity control are strongly interlocked:

- The high denticity at the large rim gives access to polynuclear  $Zn^{II}$  complexes of high nuclearity (up to four metal ions).
- In acetonitrile, the first equivalent of  $Zn^{II}$  locates at the large rim in an octahedral environment made of two tridentate groups, instead of the usually preferred tris-imidazole site at the small rim.
- In mononuclear complexes, a clean *metal translocation* is observed from the large rim site to the small rim tris-imidazole site upon the addition of long primary amines, leading to a tetrahedral  $Zn^{II}$  complex with inclusion of the bound amino guest. This translocation is *chemo-selective* (amine vs nitrile).
- In mononuclear complexes, a short amine (propylamine) induces a rearrangement of the system, leading preferentially to dinuclear complexes with concomitant amino guest encapsulation between the small rim and large rim  $Zn^{II}$  ions. Therefore, a *length selectivity* is observed within the primary amine ligands.
- In polynuclear complexes, *nuclearity is under the supramolecular control* of the guest. Small guests (MeCN, propylamine) are encapsulated between the tris-

imidazole  $Zn^{II}$  complex and the octahedral complex at the large rim. Longer guests (heptylamine) disrupt the  $O_h$  binding mode, free a tridentate ligand, and allow the nuclearity to be further extended.

- In polynuclear complexes, a *guest-triggered switch of the metal binding mode* is observed. The disruption of the octahedral binding by a long guest opens a binding site in the metal coordination sphere.

Among these results, the  $Zn^{II}$  translocation is rather unusual. In most reported cases, ion translocations involve redox, pH, or light stimuli.<sup>7,17</sup> To the best of our knowledge, only one example of guest-induced translocation has been reported so far by Fabbrizzi, involving encapsulation of an imidazolate guest.<sup>18</sup> The additional length selectivity of the phenomenon arises from the specific *induced-fit* ability of the host.

The guest-induced switch of the metal binding mode is also a result of *induced fit* and recalls the strategies employed in catalytic systems to avoid self-destruction: matrix metalloproteinases hydrolytic activity is switched on by the removal of a cysteine residue that saturates the coordination sphere of the  $Zn^{II}$  active site.<sup>19</sup> It was proposed that this switch occurs as a direct result of conformational motion generated by protein–protein binding.<sup>20,21</sup> In several iron enzymes, the coordination sphere of the active site remains saturated until substrate binding triggers the release of a water molecule, thus preparing iron for  $O_2$  activation.<sup>22–24</sup>

The supramolecular similarities with the natural systems prompt us to now explore the coordination of other metal ions, especially redox-active ones. These systems also open the way to a wide range of applications that could exploit the selective  $Zn^{II}$  translocation phenomenon, as well as the guest-selective formation/breaking of the octahedral complex.

## ASSOCIATED CONTENT

### Supporting Information

Experimental section. Synthetic procedures and characterizations of  $L^{TNpy}$  and  $L^{C_4NH_2Boc}$ . Characterization of mononuclear, polynuclear complexes, and host–guest adducts. Complementary host–guest studies. This material is available free of charge via the Internet at <http://pubs.acs.org>.

## AUTHOR INFORMATION

### Corresponding Author

\*E-mail addresses: jean-noel.rebilly@parisdescartes.fr (J.-N.R.), olivia.reinaud@parisdescartes.fr (O.R.).

### Notes

The authors declare no competing financial interest.

## ACKNOWLEDGMENTS

The authors thank Assia Hessani for her help with the ESI-MS studies. This project was supported by the CNRS (Institut de Chimie), the Ministère de l'Enseignement Supérieur et de la Recherche, and the Agence Nationale pour la Recherche [Cavity-zyme(Cu) Project No. ANR-2010-BLAN-7141].

## REFERENCES

- Bertini, I.; Sigel, A.; Sigel, H. *Handbook of Metalloproteins*; Marcel Dekker: New York, 2001.
- Lippard, S. J.; Berg, J. M. *Principles of Bioinorganic Chemistry*; University Science Books: Mill Valley, CA, 1994.
- Klinman, J. P. *J. Biol. Chem.* **2006**, *281*, 3013–3016.
- Prigge, S. T.; Eipper, B. A.; Mains, R. E.; Amzel, L. M. *Science* **2004**, *304*, 864–867.



(5) Colasson, B.; Save, M.; Milko, P.; Roithova, J.; Schroder, D.; Reinaud, O. *Org. Lett.* **2007**, *9*, 4987–4990.

(6) Gramage-Doria, R.; Armspach, D.; Matt, D. *Coord. Chem. Rev.* **2013**, *257*, 776–816.

(7) Colasson, B.; Le Poul, N.; Le Mest, Y.; Reinaud, O. *J. Am. Chem. Soc.* **2010**, *132*, 4393–4398.

(8) Rebilly, J. N.; Bistri, O.; Colasson, B.; Reinaud, O. *Inorg. Chem.* **2012**, *51*, 5965–5974.

(9) Lee, B.-Y.; Park, S. R.; Jeon, H. B.; Kim, K. S. *Tetrahedron Lett.* **2006**, *47*, 5105–5109.

(10) Colasson, B.; Reinaud, O. *J. Am. Chem. Soc.* **2008**, *130*, 15226–15227.

(11) Menard, N.; Reinaud, O.; Colasson, B. *Chem.—Eur. J.* **2013**, *19*, 642–653.

(12) The term “funnel complex” is coined according to the shape of the complex. Zn<sup>II</sup> is bound in a distorted tetrahedral environment at the small rim, to three imidazoles and a fourth labile site oriented inside the cavity. Coordination “freezes” the macrocycle in a conformation corresponding to a truncated cone, or funnel. The guest must go through the funnel for exchange and interaction at the metal center.

(13) Sénèque, O.; Giorgi, M.; Reinaud, O. *Supramol. Chem.* **2003**, *15*, 573.

(14) Sénèque, O.; Rager, M. N.; Giorgi, M.; Reinaud, O. *J. Am. Chem. Soc.* **2000**, *122*, 6183–6189.

(15) All four protons (ortho, para, meta, and meta') of the two distinct bound pyridine groups could be distinguished and identified by COSY experiments at 275 K. At 340 K, they merged in coalescence two by two to give a single peak for each position (para, meta, and meta'). The ortho protons could not be detected at this temperature. Indeed, due to the corresponding very large chemical shift difference at 275 K ( $\Delta d = 1.56$  ppm), the coalescence temperature is higher.

(16) Kano, K.; Kondo, M.; Inoue, H.; Kitagishi, H.; Colasson, B.; Reinaud, O. *Inorg. Chem.* **2011**, *50*, 6353–6360.

(17) Bofinger, R.; Ducrot, A.; Jonusauskaite, L.; McClenaghan, N. D.; Pozzo, J.-L.; Sevez, G.; Vives, G. *Aust. J. Chem.* **2011**, *64*, 1301–1314.

(18) Fabbrizzi, L.; Foti, F.; Patroni, S.; Pallavicini, P.; Taglietti, A. *Angew. Chem., Int. Ed.* **2004**, *43*, 5073–5077.

(19) Springman, E. B.; Angleton, E. L.; Birkedal-Hansen, H.; Van Wart, H. E. *Proc. Natl. Acad. Sci. U.S.A.* **1990**, *87*, 364–368.

(20) Parkin, G. *Chem. Rev.* **2004**, *104*, 699–768.

(21) Rosenblum, G.; Meroueh, S.; Toth, M.; Fisher, J. F.; Fridman, R.; Mobashery, S.; Sagi, I. *J. Am. Chem. Soc.* **2007**, *129*, 13566–13574.

(22) Costas, M.; Mehn, M. P.; Jensen, M. P.; Que, L. *Chem. Rev.* **2004**, *104*, 939–986.

(23) Elkins, J. M.; Ryle, M. J.; Clifton, I. J.; Hotopp, J. C. D.; Lloyd, J. S.; Burzlaff, N. L.; Baldwin, J. E.; Hausinger, R. P.; Roach, P. L. *Biochemistry* **2002**, *41*, 5185–5192.

(24) Denisov, I. G.; Makris, T. M.; Sligar, S. G.; Schlichting, I. *Chem. Rev.* **2005**, *105*, 2253–2277.